Cognitive Neurodynamics (2021) 15:265–277
https://doi.org/10.1007/s11571-020-09596-4

RESEARCH ARTICLE

# Energy dependence on discharge mode of Izhikevich neuron driven by external stimulus under electromagnetic induction

Yumei Yang[1] · Jun Ma[2,3] · Ying Xu[1] · Ya Jia[1]

Received: 24 December 2019 / Revised: 14 March 2020 / Accepted: 1 April 2020 / Published online: 11 May 2020
© Springer Nature B.V. 2020

**Abstract**
Energy supply plays a key role in metabolism and signal transmission of biological individuals, neurons in a complex electromagnetic environment must be accompanied by the absorption and release of energy. In this paper, the discharge mode and the Hamiltonian energy are investigated within the Izhikevich neuronal model driven by external signals in the presence of electromagnetic induction. It is found that multiple electrical activity modes can be observed by changing external stimulus, and the Hamiltonian energy is more dependent on the discharge mode. In particular, there is a distinct shift and transition in the Hamiltonian energy when the discharge mode is switched quickly. Furthermore, the amplitude of periodic stimulus signal has a greater effect on the neuronal energy compared to the angular frequency, and the average Hamiltonian energy decreases when the discharge rhythm becomes higher. Based on the principle of energy minimization, the system should choose the minimum Hamiltonian energy when maintaining various trigger states to reduce the metabolic energy of signal processing in biological systems. Therefore, our results give the possible clues for predicting and selecting appropriate parameters, and help to understand the sudden and paroxysmal mechanisms of epilepsy symptoms.

**Keywords** Izhikevich neuronal model · Electromagnetic induction · Mixed mode · Hamiltonian energy

## Introduction

The dynamic behavior of neurons is particularly important for understanding information encoding and related diseases in the nervous system, therefore, some reliable biological neuron models have been proposed and improved to explore the occurrence mechanisms of action potential. The most familiar neuron model is the Hodgkin–Huxley model proposed by Hodgkin and Huxley (1952), and some simplified models that can exhibit the characteristics of electrical activities in neurons have also been proposed subsequently (FitzHugh 1961; Wilson 1999; Morris and Lecar 1981; Hindmarsh and Rose 1982). Based on different neuron models, many interesting works have been carried out on estimating various dynamic behaviors in single neuron or neural network affected by various internal or external factors (e.g. noise, temperature, synapse, input signal). For instance, the response of neurons or neural networks to weak signal can be maximized under appropriate noise (Zhao et al. 2016; Yao and Ma 2018). The electrical activities can change significantly under the influence of temperature (Lu et al. 2019c; Xu et al. 2019b). Wave propagation can be realized by adjusting synaptic weight and synaptic characteristic time in a feed-forward neural network (Ma et al. 2015; Ge et al. 2018). The electrical activity patterns of single neuron and neural network are affected by ion channel blocks (Xu et al.

✉ Ya Jia
jiay@mail.ccnu.edu.cn

Yumei Yang
yangym@mails.ccnu.edu.cn

Jun Ma
hyperchaos@163.com

Ying Xu
xuyingny@mails.ccnu.edu.cn

[1] Department of Physics, Central China Normal University, Wuhan 430079, China

[2] Department of Physics, Lanzhou University of Technology, Lanzhou 730050, China

[3] School of Science, Chongqing University of Posts and Telecommunications, Chongqing 430065, China

2018a). The strength and frequency of network synchronization will vary with the combination of network self-synchronization frequency and input signal frequency (Lv et al. 2014).

In recent years, electromagnetic induction induced by the fluctuation of membrane potential or the distribution of ion concentration have been introduced into the research of neurons and neural networks. For example, the mode transformation of electrical activities in single neuron under electromagnetic induction has been investigated (Lv and Ma 2016; Xu et al. 2017; Mondal et al. 2019; Liu et al. 2019). The synchronization between coupled neurons under electromagnetic induction has been studied (Ma et al. 2017; Xu et al. 2018b). The effects of electromagnetic induction on spiral waves formation and signal propagation in neural networks have been discussed (Rostami and Jafari 2018; Ge et al. 2019a, b). The effects of electromagnetic field coupling on the spiking activities of neural network have been investigated (Xu et al. 2019a). In order to approximate the real environment of the nervous system, which means more realistic input, various external signals were applied to neurons or neuron networks. For instance, the propagation of biological weak signals was discussed in neural networks (Lu et al. 2019a; Ge et al. 2020a). The sinusoidal periodic signals were used to study the response of electrical activities in single neuron or neural networks (Guo and Li 2009; Farokhniaee and Large 2017). The high-low frequency signal mixed with a high frequency periodic signal and a low frequency periodic signal was imposed on the neurons to investigate vibrational resonance phenomenon (Zaikin et al. 2002; Ullner et al. 2003), but the electromagnetic induction was not taken into account. In fact, neurons can be regarded as excitable media, and the fluctuation in neuronal membrane potential alters the distribution of electromagnetic field inside and outside neurons (Lv et al. 2016). In addition, the polarization and magnetization are triggered when the neuron is exposed to external field or electromagnetic radiation (Parastesh et al. 2018). Therefore, the electromagnetic induction and radiation should be considered for neurons, and the electrical activities of neurons will be adjusted under feedback effect. Besides, the application of high-low frequency signal is actually universal in neural system. For example, bursting neurons may show two widely distinct time scales, because the high frequency and low frequency signals correspond to different input channels in a neuron, respectively. Moreover, the beneficial role of high frequency stimulation has been found in previous researches, such as the increased absorption of drugs by brain cells, the improvement of muscle healing, or the treatment of Parkinson's disease and other disorders in neuronal activity (Gong and Xu 2001). Recently, some researchers have discussed the electrical activities of neurons when both electromagnetic induction and high-low frequency signal exist (Lu et al. 2020; Ge et al. 2020b). The results from previous studies have shown that both electromagnetic induction and high-low frequency signal have significant effects on the dynamic behavior of neurons.

Energy supply plays a key role in metabolism and signal transmission of biological individuals (Laughlin and Sejnowski 2003). The research on the energy supply and consumption of nervous system has been done in experiments, and it needs to be further explored in quantitative theoretical analysis. The generation of action potential and the transition of discharge modes are related to energy coding (Wang and Zhang 2007; Wang et al. 2009), and the electrical activities of single neuron and neural network can be expressed by energy (Wang and Zhu 2016; Wang et al. 2015b). There are still some difficulties in accurately detecting energy supply and consumption, but the energy expenditure in electrical activity can be estimated by some computational methods based on neuron models. For instance, the biological energy consumed by Na/K-ATPase pumps was calculated based on the Chay neuron model, and it was found that the energy expenditure in busting state is minimal (Zhu et al. 2019). The Hamiltonian energy was calculated based on Hindmarsh-Rose neuron model according to Helmholtz theorem, and it was shown that the energy depends on the discharge activity (Song et al. 2015; Wang et al. 2016). When neurons are stimulated by external signals, the corresponding neural energy will change with the conversion of action potential, and the unique relationship between membrane potential and energy was discussed (Wang et al. 2015a, 2018). Due to the scalar feature of energy, the dynamic response of neural model can describe the pattern of neural coding through energy superposition whether it is based on single neuron, neural populations or networks (Zhu et al. 2018; Wang and Wang 2014; Wang et al. 2008). Moreover, neural energy may be an effective way to study the behavior of brain activity, which can further investigate cognitive activity (Wang et al. 2017b). Extensive investigations found that the Hamiltonian energy is regulated by external signals (Wang et al. 2017a; Lu et al. 2019b; Wu et al. 2019). The Hamiltonian energy calculated from the dimensionless nonlinear dynamical system can provide useful clues to better understand the relationship between discharge mode and energy coding.

In this paper, considering the electromagnetic induction, the improved Izhikevich neuron model driven by external current or external electromagnetic radiation is described respectively in the "Models and methods" section, and the Hamiltonian energy function associated with the improved model is deduced according to Helmholtz theorem. Then, the transformation of electrical activity and Hamiltonian energy is discussed and analyzed in the "Numerical results

and discussions" section. Finally, the results of our work are summarized, and the possible further applications are discussed in the "Conclusions" section.

## Models and methods

The Izhikevich neuronal model (Izhikevich 2003, 2004) combines the biological rationality and the computational efficiency, which can reproduce a large number of electrical activities of cortical neurons. To our knowledge, the fluctuation in neuronal membrane potential can induce electromagnetic induction, and the magnetic flux across the membrane may be changed. In addition, the variation of magnetic flux also changes the membrane potential. Therefore, the influence of electromagnetic induction is considered by using a magnetic flux variable, and the feedback of magnetic flux to membrane potential is realized through memristor. According to Maxwell's electromagnetic induction theorem (Carpenter 1999), the improved Izhikevich model driven by the external periodic current or the external high-low frequency electromagnetic radiation is given in the following two parts, respectively.

(1) The improved Izhikevich model driven by external stimulus current

Considering electromagnetic induction, the dynamic equation of single Izhikevich neuron model driven by external stimulus current is described as follows:

$$\begin{cases} \dfrac{dv}{dt} = 0.04v^2 + 5v + 140 - u - k\rho(\phi)v + I + I_{ext}, \\ \dfrac{du}{dt} = a(bv - u), \\ \dfrac{d\phi}{dt} = k_1 v - k_2\phi, \end{cases} \tag{1}$$

with the auxiliary after-spike resetting

$$\text{if } v \geq 30 \text{ mV, then } \begin{cases} v \leftarrow c, \\ u \leftarrow u + d, \end{cases} \tag{2}$$

where the variables $v$, $u$ and $\varphi$ describe the membrane potential of the neuron, membrane recovery variable associated with the activation of $K^+$ currents and the inactivation of $Na^+$ currents, and the magnetic flux across the neuronal membrane, respectively. Parameter $a$ is the recovery constant, $b$ describes the susceptibility of the recovery variable to the subthreshold fluctuation of membrane potential, $c$ is the reset value of membrane potential when the voltage reaches 30 mV, and $d$ describes the after-spike behavior associated with the recovery variable. The term $k\rho(\varphi)v$ is the feedback current associated with electromagnetic induction, $k_1 v$ describes the effect induced by membrane potential on magnetic flux, and $k_2\varphi$ represents the magnetic leakage. $I$ is the constant current, and $I_{ext} = A\sin(\omega t)$ is the external forcing current, which directly affects the membrane potential under fixed parameters or external forcing.

Memristor is the fourth fundamental circuit element that connects the flux with charge. According to the characteristics of memristor (Chua 1971; Strukov et al. 2008), the magnetic flux-controlled memory conductance is estimated by

$$\rho(\phi) = \frac{dq(\phi)}{d\phi} = \alpha + 3\beta\phi^2, \tag{3}$$

where $\alpha$ represents constant conductance, $\beta$ indicates the feedback rate of magnetic flux, both of which depend on the memristor, and $q(\varphi)$ is the magnetic flux-related charge across the memristor.

The absorption and release of energy during the transition of electrical activity is worth investigating. According to Helmholtz's theorem (Kobe 1986), the neuron's dynamical equations can be viewed as a velocity vector field and further decomposed into the sum of two sub-vector fields $\mathbf{f}(*) = \mathbf{f}_c(*) + \mathbf{f}_d(*)$, where $\mathbf{f}_c(*)$ is the vortex field containing the full rotation and $\mathbf{f}_d(*)$ is the gradient field containing the divergence. Therefore, the Hamilton energy of the improved Izhikevich neuron model can be calculated.

The two sub-vector fields in Eq. (1) are rewritten as following:

$$\begin{pmatrix} \dfrac{dv}{dt} \\ \dfrac{du}{dt} \\ \dfrac{d\phi}{dt} \end{pmatrix} = \mathbf{f}_c(v,u,\phi) + \mathbf{f}_d(v,u,\phi), \tag{4}$$

with

$$\mathbf{f}_c(v,u,\phi) = \mathbf{J}(v,u,\phi)\cdot\nabla H = \begin{pmatrix} 140 - u + I + I_{ext} - \phi \\ abv \\ k_1 v \end{pmatrix},$$

$$\mathbf{f}_d(v,u,\phi) = \mathbf{R}(v,u,\phi)\cdot\nabla H = \begin{pmatrix} 0.04v^2 + 5v - k\rho(\phi)v + \phi \\ -au \\ -k_2\phi \end{pmatrix},$$

where $H$ is the Hamilton energy function, and $\mathbf{J}(v,u,\varphi)$ and $\mathbf{R}(v,u,\varphi)$ are the skew-symmetric matrix and the symmetric matrix, respectively.

The Hamilton energy function $H$ associated with Eqs. (1) and (4) is calculated by

$$\begin{cases} \nabla H^T \mathbf{f}_c(v,u,\phi) = 0, \\ \nabla H^T \mathbf{f}_d(v,u,\phi) = dH/dt, \end{cases} \tag{5}$$

where the super index $T$ represents the transpose of matrix. By substituting Eq. (4) into Eq. (5), we have

$$(140 - u + I + I_{ext} - \phi)\frac{\partial H}{\partial v} + (abv)\frac{\partial H}{\partial u} + (k_1 v)\frac{\partial H}{\partial \phi} = 0. \tag{6}$$

The general solution of Eq. (6) is

$$H = (140 - u + I + I_{ext} - \phi)^2 + abv^2 + k_1 v^2. \tag{7}$$

Furthermore, the differential coefficient of Hamilton energy versus time is obtained from

$$\begin{aligned} \frac{dH}{dt} &= 2(140 - u + I + I_{\text{ext}} - \phi)\,(-abv + au - k_1 v + k_2\phi) \\ &\quad + (2abv + 2k_1 v)\,\left(0.04v^2 + 5v + 140 - u - k\rho(\phi)v \right. \\ &\quad \left. + I + I_{ext}\right) \\ &= \nabla H^T \mathbf{f}_d. \end{aligned} \tag{8}$$

Therefore, the Hamilton energy function as shown in Eq. (7) is a reliable solution of Eq. (6).

(2) The improved Izhikevich model driven by external electromagnetic radiation

Considering electromagnetic induction, the dynamic equation of single Izhikevich neuron model driven by electromagnetic radiation is described as following:

$$\begin{cases} \frac{dv}{dt} = 0.04v^2 + 5v + 140 - u - k\rho(\phi)v + I, \\ \frac{du}{dt} = a(bv - u), \\ \frac{d\phi}{dt} = k_1 v - k_2\phi + \phi_{ext}, \end{cases} \tag{9}$$

with the auxiliary after-spike resetting

$$\text{if } v \geq 30 \text{ mV, then } \begin{cases} v \leftarrow c, \\ u \leftarrow u + d, \end{cases} \tag{10}$$

where $\varphi_{ext} = A\cos(\omega t) + B\cos(N\omega t)$ represents the influence of external field or electromagnetic radiation, which alters magnetic flux distribution and affects the membrane potential under a specific function. $A$ and $B$ are the amplitudes of high-low frequency signal, $\omega$ and $N\omega$ are the angular frequencies. In this case, the two sub-vector fields of Eq. (9) are written as follows:

$$\mathbf{f}_c(v,u,\phi) = \mathbf{J}(v,u,\phi)\nabla H = \begin{pmatrix} 140 - u + I - \phi \\ abv \\ k_1 v + \phi_{ext} \end{pmatrix},$$
$$\mathbf{f}_d(v,u,\phi) = \mathbf{R}(v,u,\phi)\nabla H = \begin{pmatrix} 0.04v^2 + 5v - k\rho(\phi)v + \phi \\ -au \\ -k_2\phi \end{pmatrix}. \tag{11}$$

Similarly, by substituting Eq. (11) into Eq. (5), we have

$$(140 - u + I - \phi)\frac{\partial H}{\partial v} + (abv)\frac{\partial H}{\partial u} + (k_1 v + \phi_{ext})\frac{\partial H}{\partial \phi} = 0. \tag{12}$$

The general solution of Eq. (12) is

$$H = (140 - u + I - \phi)^2 + abv^2 + k_1 v^2 + 2\phi_{ext} v. \tag{13}$$

Therefore, the differential coefficient of Hamilton energy versus time can be obtained from

$$\begin{aligned} \frac{dH}{dt} &= 2(140 - u + I - \phi)\,(-abv + au - k_1 v + k_2\phi - \phi_{ext}) \\ &\quad + 2(abv + k_1 v + \phi_{ext})\,\left(0.04v^2 + 5v + 140 - u \right. \\ &\quad \left. - k\rho(\phi)v + I\right) \\ &= \nabla H^T \mathbf{f}_d. \end{aligned} \tag{14}$$

As a result, Eq. (13) is also a reliable solution of Eq. (12).

In our numerical simulation, the Euler algorithm is used, and the time step is set as 0.001. According to most of the previous works, some parameter values are always set to the same, such as $a$ = 0.02, $b$ = 0.2, $c$ = − 65, $d$ = 8, $I$ = 10, Besides, $k$ = 0.01, $k_1$ = 0.01, $k_2$ = 0.2, $\alpha$ = 0.4, $\beta$ = 0.02 are selected as the appropriate parameter value related to electromagnetic induction, and the initial values are set as ($v_0$, $u_0$, $\varphi_0$) = (0.3, 0.2, 0.1). The selection of system mode has nothing to do with the selection of initial value.

## Numerical results and discussions

The process of injecting external stimuli is the process of injecting energy, the generation of action potential and the transition of discharge mode must be accompanied by the supply and consumption of energy. Therefore, we investigate and analyze the transformation of electrical activity and Hamiltonian energy within the improved Izhikevich neuron under different external stimuli in this section.

(1) Effects of the external stimulus current

As shown in Fig. 1, the sample time series of membrane potential and energy function are calculated during

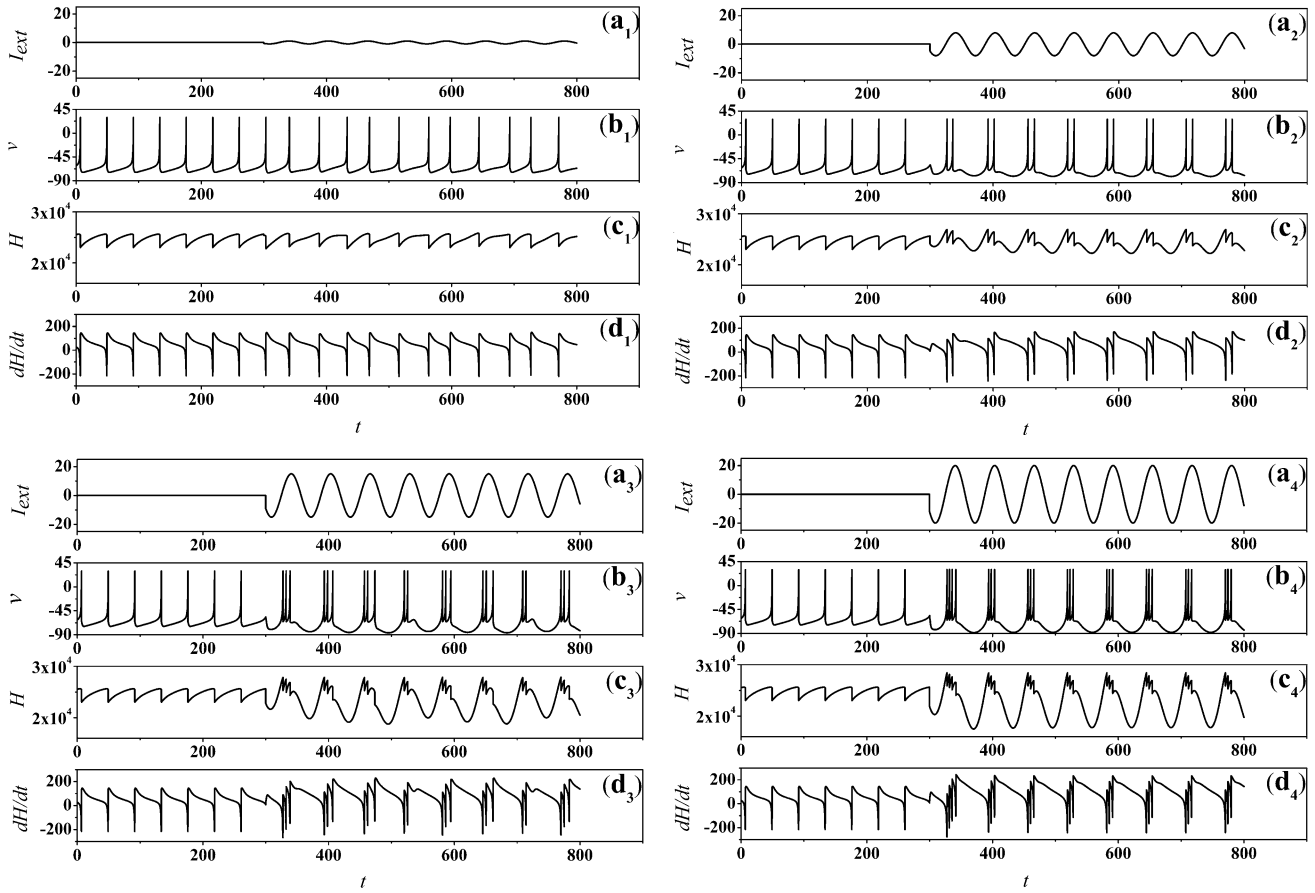


**Fig. 1** Sample time series of membrane potential in Eq. (1) and energy function in Eq. (7) by applying external stimulus current at $\omega = 0.1$. For $(\mathbf{a_1})$–$(\mathbf{d_1})$ $A = 1.0$; $(\mathbf{a_2})$–$(\mathbf{d_2})$ $A = 8.0$; $(\mathbf{a_3})$–$(\mathbf{d_3})$ $A = 15.0$; $(\mathbf{a_4})$–$(\mathbf{d_4})$ $A = 20.0$, stimulus $I_{ext} = A\sin(\omega t)$

different amplitudes of driving current. The transient period is selected as 800 time units, and the external stimulus $I_{ext} = A\sin(\omega t)$ is added at $t = 300$ time units. It can be seen that when the angular frequency is fixed, the neuron exhibits multiple discharge patterns by changing the amplitude, and the fluctuation of energy function depends on the electric activities.

It is found that the electric activity changes from regular spiking state into complex chaotic state at $t = 300$ time units when the amplitude $A = 1.0$, and the variation of Hamiltonian energy also changes from regular into irregular. When the value of $A$ is set as 8.0, the discharge mode switches from spiking to period-2 bursting, and there is a distinct shift in energy. Furthermore, the range of Hamiltonian energy in bursting state is larger than that of the spiking and chaotic states. The potential mechanism may be that the generation of bursting action potential requires more energy supply but consumes even more, that means the average energy decreases. When $A$ is set as 15.0 or 20.0, the mixed state and the period-3 bursting state are observed, respectively, and the range of Hamiltonian energy becomes larger under a larger current amplitude. Comparing these results, the average energy decreases with the increase of stimulation current amplitude. When the electrical activity switches to a high rhythm, the average energy decreases because each action potential carries a certain amount of energy and follows the law of energy conservation.

In order to reveal the overall effect of current amplitude $A$ on electrical activities, the bifurcation diagram is plotted by calculating the interspike intervals ($ISI$) of membrane potentials under different parameter values, and the results obtained by program are shown in Fig. 2a. It is found that the discharge patterns show some regular changes when the amplitude exceeds certain value. In our numerical simulation results, the electrical activity presents chaotic state when the value of $A$ is smaller than 1.624, and it presents alternating transformation between bursting state and mixed state when the value of $A$ is larger than 1.624. Furthermore, the average Hamiltonian energy function is calculated in a transient period $T = 2000$ time units as shown in Fig. 2b. A large number of numerical calculation results prove that the statistical properties of average Hamiltonian energy have little to do with the choice of calculation time $T$. Here, the average Hamiltonian energy function is calculated by the following formula

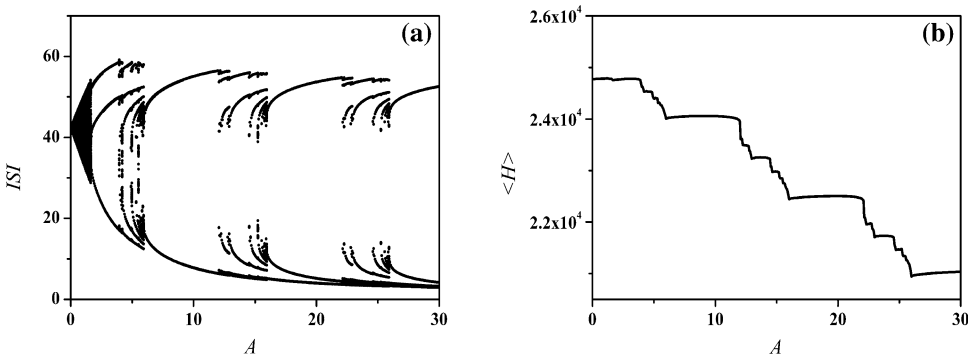


**Fig. 2** **a** Bifurcation diagram associated with the amplitude of external stimulus current. **b** Evolution of the average energy function with the amplitude of external stimulus current. Stimulus $I_{ext} = A\sin(\omega t)$ with $\omega = 0.1$

$$\langle H \rangle = \int_{t_0}^{t_0+T} H(v, u, \phi)dt/T, \tag{15}$$

where $t_0$ and $T$ are the initial time and period for calculating the average Hamiltonian energy, respectively, the energy function is described by Eq. (7) or Eq. (13) in this paper.

It is interesting that the average energy function curve shows a step-like decline with the increase of stimulus current amplitude. Comparing Fig. 2a with Fig. 2b, which illustrates that the energy depends on the discharge mode. The horizontal lines of the average energy function curve are related to the increase and decrease of interspike intervals symmetrically, the average firing rate does not change and the average energy does not change. The descending lines of the curve are related to the changes with a higher discharge rhythm, the average energy carried by each action potential decreases due to the restriction of energy conservation.

Figure 3 shows the evolution of membrane potential and Hamiltonian energy over time at different angular frequencies of driving current. When external stimulation is added, the electrical activity changes from regular spiking state into period-3 and period-2 discharge state at $\omega = 0.05$ and $\omega = 0.08$, respectively. The electrical activity mode is mixed state when the value of $\omega$ is 0.12, and it is period-1 firing when the value of $\omega$ is 0.15. In addition, there is a quick transition in energy when external stimulation is added at $t = 300$ time units. But unlike the results in Fig. 1, the fluctuation range of energy does not always increase with the increase of angular frequency as shown in Fig. 3, so the average energy does not always decrease. Similarly, in order to investigate the global effect of angular frequency on the electrical activities and energy function, the bifurcation diagram and average energy function associated with different angular frequencies are plotted as shown in Fig. 4.

Figure 4a shows that the electrical activities of neuron can present rich discharge patterns with the change of angular frequency when periodic forcing current is applied to the neuron. When the value of angular frequency $\omega$ is less than 0.018, the discharge mode is chaotic, and when the value of $\omega$ is greater than 0.018, the periodicity of the electrical activities becomes obvious. This is somewhat similar to the trend of increasing the amplitude of stimulation current. However, according to the results in Fig. 4b, the changes in average energy are different from the results of increasing current amplitude. The average energy function curve shows a wave-like decline with the increase of current angular frequency. Comparing Fig. 4a with Fig. 4b, the Hamiltonian energy still depends on the electrical activity mode. The average energy in chaotic state fluctuates only slightly with the change of angular frequency, the rising lines of average energy curve correspond to the process from high rhythm discharge to low rhythm discharge, and the descending lines of average energy curve correspond to the process from low rhythm discharge to high rhythm discharge. The characteristics of this curve are also consistent with the results in Fig. 3.

(2) Effects of the external electromagnetic radiation

The electrical activity and energy of neurons in reality are more or less affected by external electromagnetic field. Indeed, the external radiation is estimated within the magnetic flux variable, and applying disturbance on the magnetic flux variable indicates potential energy injection and release, which is fully confirmed by Eq. (13). Figure 5 shows the evolution of membrane potential and Hamiltonian energy over time at different low frequency amplitudes. The external electromagnetic radiation is described as $\varphi_{ext} = A\cos(\omega t) + B\cos(N\omega t)$. In order to better observe the phenomenon, the transient period is selected as 600 time units, and the high-low frequency stimulation signal is added at $t = 200$ time units in this part. The parameter values of electromagnetic radiation are fixed as ($B$, $\omega$, $N$) = (3.0, 0.3, 10) in Fig. 5. It is showed that the increase of low frequency amplitude $A$ can lead to various discharge activities, and the firing rate increases obviously. In addition, the fluctuation range of Hamiltonian energy becomes larger by increasing the value of $A$.

Figure 6a shows the bifurcation diagram associated with the low frequency amplitude of electromagnetic radiation.

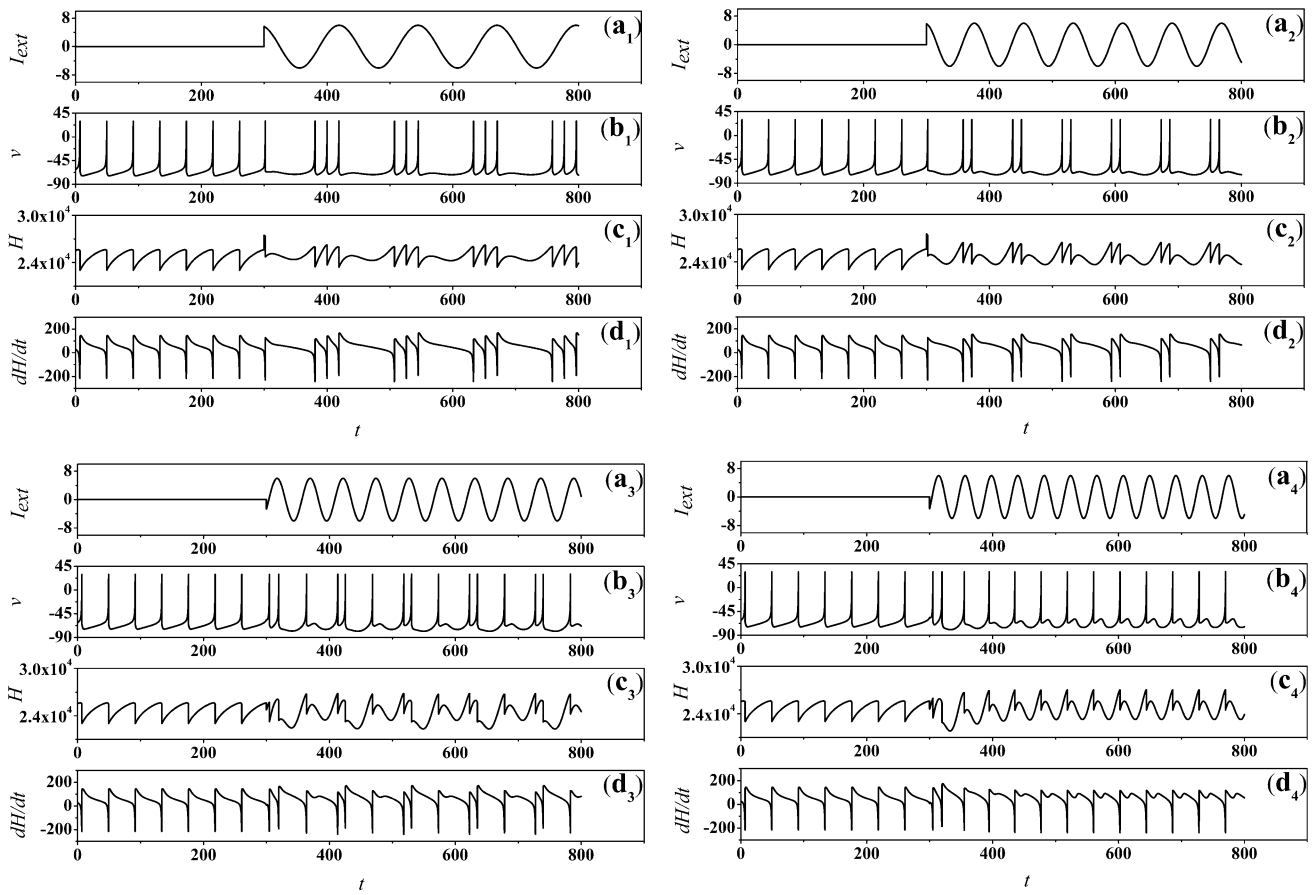


**Fig. 3** Sample time series of membrane potential in Eq. (9) and energy function in Eq. (13) by applying external stimulus current at $A = 6.0$. For $(\mathbf{a_1})$–$(\mathbf{d_1})$ $\omega = 0.05$; $(\mathbf{a_2})$–$(\mathbf{d_2})$ $\omega = 0.08$; $(\mathbf{a_3})$–$(\mathbf{d_3})$ $\omega = 0.12$; $(\mathbf{a_4})$–$(\mathbf{d_4})$ $\omega = 0.15$, stimulus $I_{ext} = A\sin(\omega t)$

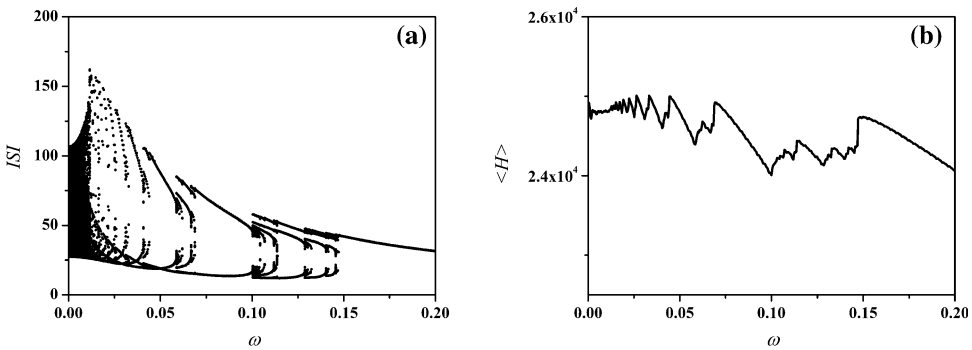


**Fig. 4** **a** Bifurcation diagram associated with the angular frequency of external stimulus current. **b** Evolution of the average energy function with the angular frequency of external stimulus current. Stimulus $I_{ext} = A\sin(\omega t)$ with $A = 6.0$

Comparing Fig. 6a with Fig. 2a, it is found that the transition of firing patterns under high-low frequency electromagnetic radiation is more complicated than that under periodic current stimulation. This phenomenon indicates that the complex external electromagnetic radiation environment may have a greater impact on the electrical activity of neurons. Similarly, the average Hamiltonian energy of neurons under electromagnetic radiation is investigated, which is calculated by Eq. (15) in a transient period $T = 2000$ time units. the average energy function curve in Fig. 6b also shows a step-like decline similar to Fig. 2b. But the average energy curve here is steeper, which means that energy changes faster, and neurons are more sensitive to external electromagnetic radiation compared to external current stimulation. Comparing Fig. 6a with Fig. 6b, the relatively horizontal lines of average energy curve correspond to the state in which the discharge rhythm remains unchanged, and the relatively steep lines are related to the high discharge rhythm. The results in Fig. 6 demonstrate that energy depends on the discharge mode under electromagnetic radiation, and the energy

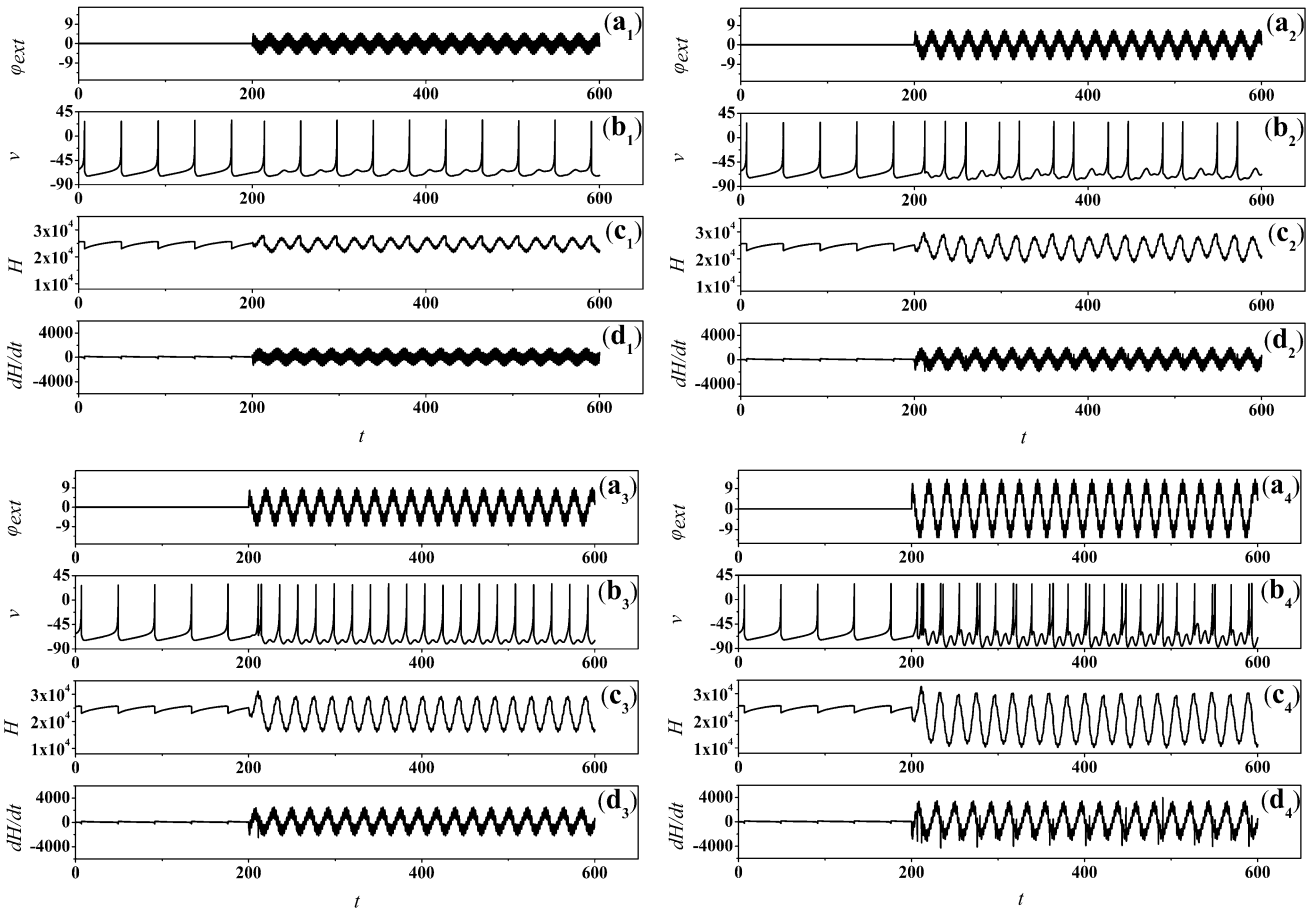


**Fig. 5** Sample time series of membrane potential in Eq. (9) and energy function in Eq. (13) by applying external electromagnetic radiation at $B = 3.0$, $\omega = 0.3$, $N = 10$. For $(\mathbf{a_1})$–$(\mathbf{d_1})$ $A = 2.0$; $(\mathbf{a_2})$–$(\mathbf{d_2})$ $A = 4.0$; $(\mathbf{a_3})$–$(\mathbf{d_3})$ $A = 6.0$; $(\mathbf{a_4})$–$(\mathbf{d_4})$ $A = 10.0$, stimulus $\varphi_{ext} = A\cos(\omega t) + B\cos(N\omega t)$

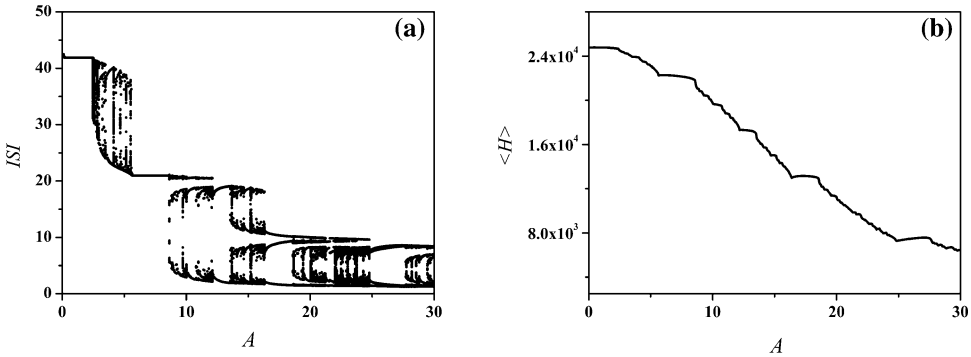


**Fig. 6** **a** Bifurcation diagram associated with the low frequency amplitude of electromagnetic radiation. **b** Evolution of the average energy function with the low frequency amplitude of electromagnetic radiation. External stimulus $\varphi_{ext} = A\cos(\omega t) + B\cos(N\omega t)$ with $B = 3.0$, $\omega = 0.3$, $N = 10$

decreases with a higher discharge rhythm, which is consistent with the results under current stimulation.

Figure 7 shows the evolution of membrane potential and energy function over time under different high frequency amplitudes. External high-low frequency electromagnetic radiation parameters are fixed as $(A, \omega, N) = (3.0, 0.3, 10)$. the neuron exhibits period-3 firing when the high frequency amplitude $B$ is set as 5.0, and switches to period-5 firing when $B$ is set as 16.0. It is period-7 firing when the value of $B$ is selected as 19.0, and it is period-2 firing when the value of $B$ is selected as 25.0. The fluctuation range of energy increases with the transition of discharge mode. The results in Fig. 7 illustrate that the high frequency amplitude $B$ of electromagnetic radiation also has some effects on the electrical activity mode and energy.

Figure 8 reveals the global effect of high frequency amplitude $B$ on electric activity mode and energy. From Fig. 8a, there is a clearly denser area, which divides the

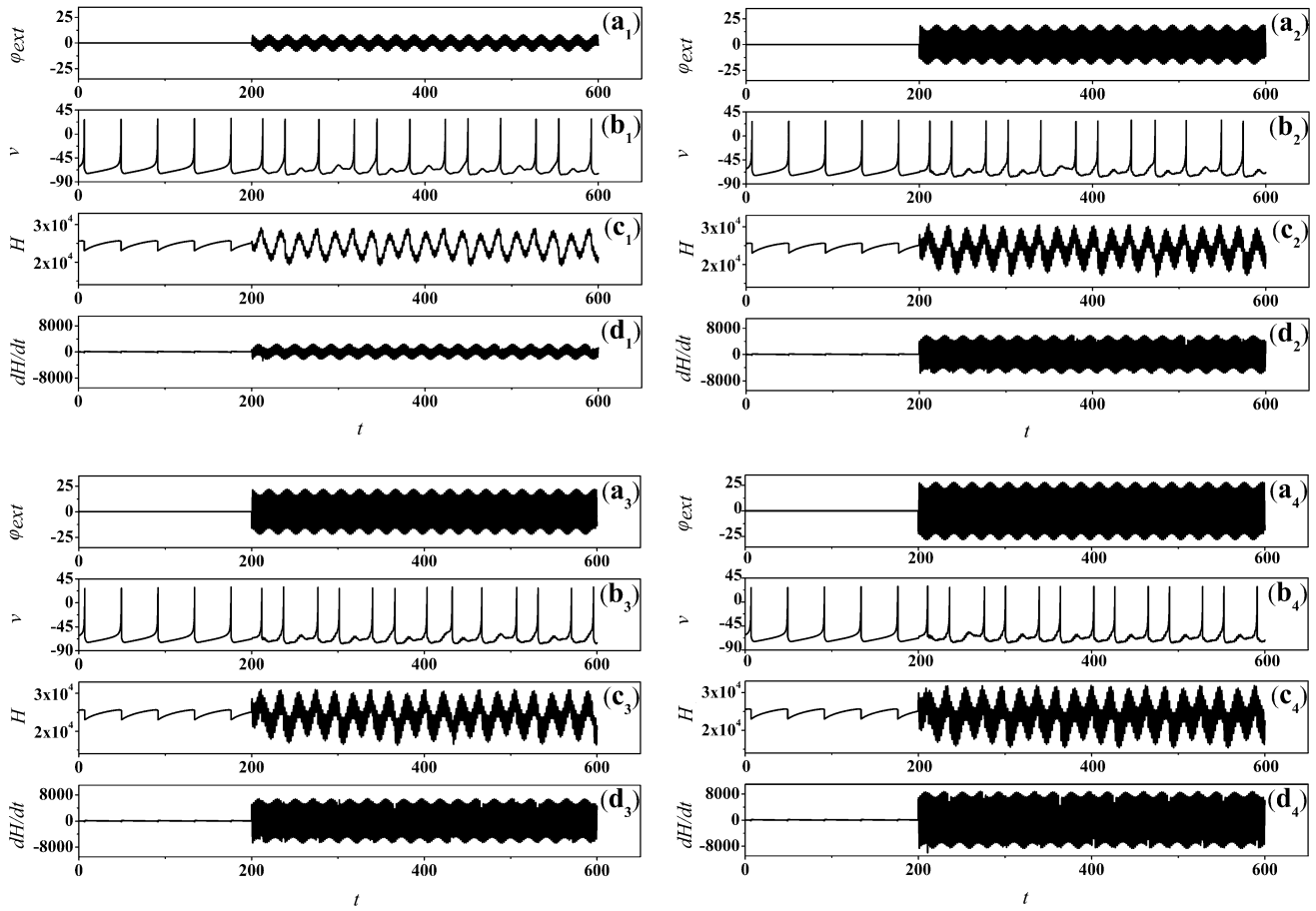


**Fig. 7** Sample time series of membrane potential in Eq. (9) and energy function in Eq. (13) by applying external electromagnetic radiation at $A = 3.0$, $\omega = 0.3$, $N = 10$. For $(\mathbf{a_1})$–$(\mathbf{d_1})$ $B = 5.0$; $(\mathbf{a_2})$–$(\mathbf{d_2})$ $B = 16.0$; $(\mathbf{a_3})$–$(\mathbf{d_3})$ $B = 19.0$; $(\mathbf{a_4})$–$(\mathbf{d_4})$ $B = 25.0$, stimulus $\varphi_{ext} = A\cos(\omega t) + B\cos(N\omega t)$

bifurcation diagram into three areas roughly. When the value of $B$ is less than 13.4, it is period-3 firing. When the value of $B$ is greater than 22.2, it is period-2 firing. When the value of $B$ is between 13.4 and 22.2, the periodic discharge and chaotic discharge change alternately. From Fig. 8b, it shows that the average energy curve associated with the high frequency amplitude $B$ can also be roughly divided into three parts: the smooth part that drops slowly, the non-smooth part that drops rapidly, and the smooth part that has a hillside. Comparing Fig. 8a with Fig. 8b, the average energy drops suddenly when the discharge mode changes from periodic state into chaotic state, and the average energy no longer drops or even rises when the discharge mode changes from chaotic state into periodic state. This phenomenon further proves that the average energy decreases in a high rhythm discharge state, which is consistent with those discussed above. By comparing Fig. 8 with Fig. 6, we draw a conclusion that the influence

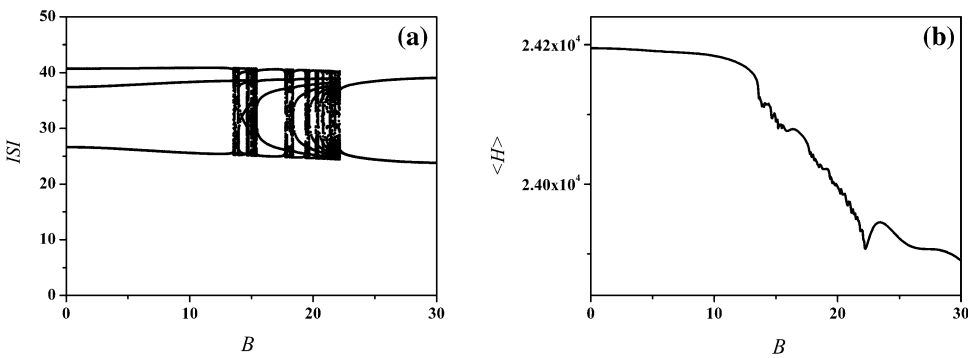


**Fig. 8** **a** Bifurcation diagram associated with the high frequency amplitude of electromagnetic radiation. **b** Evolution of the average energy function with the high frequency amplitude of electromagnetic radiation. External stimulus $\varphi_{ext} = A\cos(\omega t) + B\cos(N\omega t)$ with $A = 3.0$, $\omega = 0.3$, $N = 10$

of high frequency amplitude $B$ on the electrical activity and energy of neurons is smaller than that of low frequency amplitude $A$.

Figure 9 shows the sample time series of membrane potential and energy function under different angular frequencies. The parameters of external high-low frequency electromagnetic radiation are fixed as ($A$, $B$, $N$) = (3.0, 3.0, 10). As shown in Fig. 9, the neuron exhibits period-5 firing when the value of angular frequency $\omega$ is selected as 0.15. It is period-3 firing when the value of $\omega$ is selected as 0.25. It is period-1 firing when the value of $\omega$ is selected as 0.35, and it is period-2 firing when the value of $\omega$ is selected as 0.41. In addition, the fluctuation range of energy decreases as $\omega$ increases, which means that the average energy increases as $\omega$ increases. The results in Fig. 9 illustrate that the electrical activity of neuron is closely related to the angular frequency of high-low frequency electromagnetic radiation, and the energy is also closely related to the electrical activity.

Figure 10 shows the bifurcation diagram and the evolution of average Hamiltonian energy associated with the angular frequency. From Fig. 10a, with the increase of angular frequency $\omega$, the *ISI* (interspike interval) changes spirally and maintains horizontal when the value of $\omega$ exceeds certain value. The results in Fig. 10a indicate that it is easy to realize the transition of multiple discharge modes by changing angular frequency in the range of less than 0.75. From Fig. 10b, the average energy rises greatly when the high-low frequency electromagnetic radiation is added, and there is a wave-like rising curve followed by a horizontal line. The results in Fig. 10b illustrate that compared with the absence of electromagnetic radiation, the high-low frequency electromagnetic radiation can greatly increase the Hamiltonian energy of neurons, but the change of angular frequency has little effect on energy. From the results above, it is showed that neurons are more sensitive to the high-low frequency amplitudes than angular frequencies. The potential mechanism may be that the stimulus signal with a larger amplitude (or strength) can inject sufficient energy to induce multiple modes transition in electrical activities, while angular frequency only

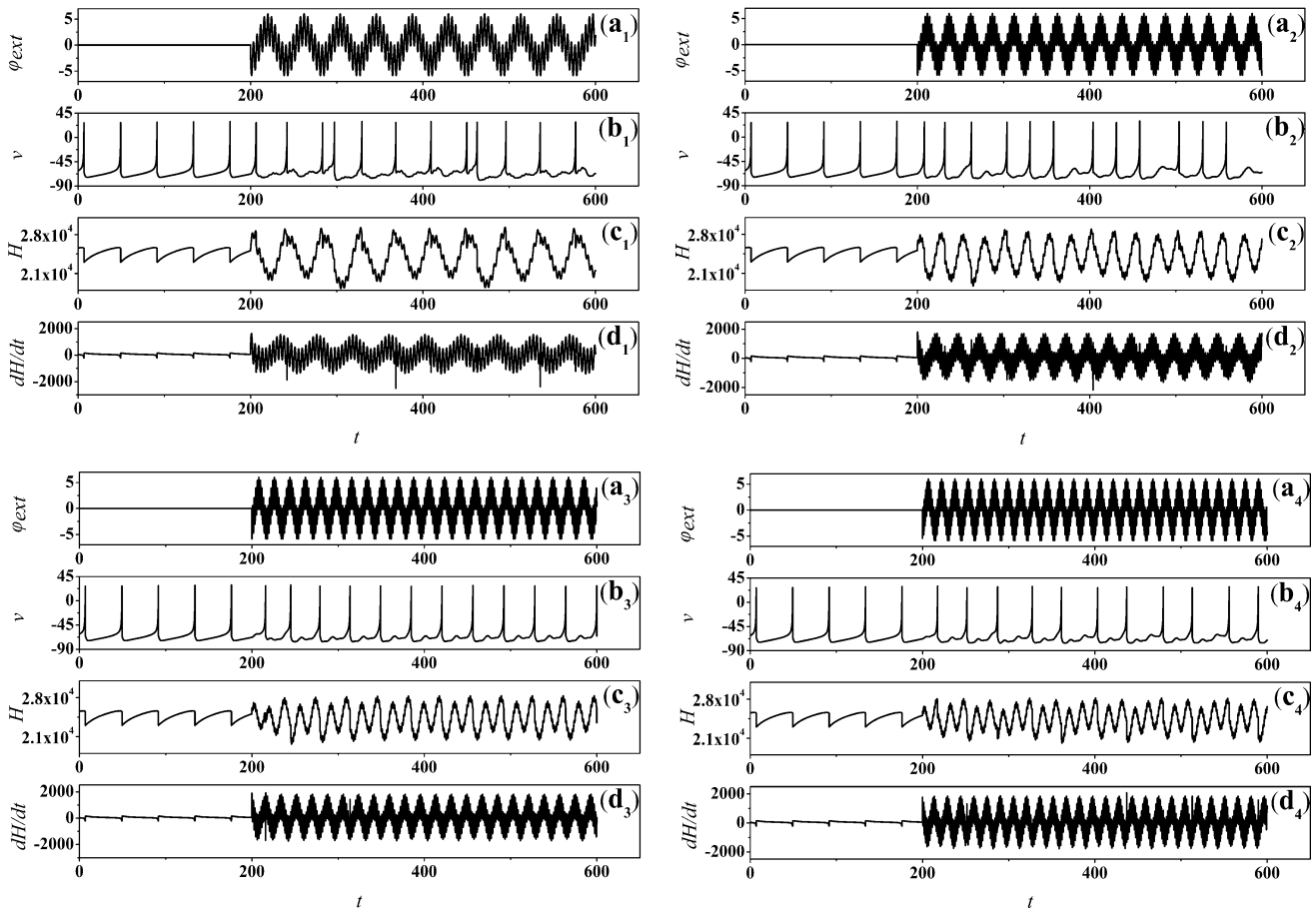


**Fig. 9** Sample time series of membrane potential in Eq. (9) and energy function in Eq. (13) by applying external electromagnetic radiation at $A$ = 3.0, $B$ = 3.0, $N$ = 10. For ($\mathbf{a_1}$)–($\mathbf{d_1}$) $\omega$ = 0.15; ($\mathbf{a_2}$)-($\mathbf{d_2}$) $\omega$ = 0.25; ($\mathbf{a_3}$)-($\mathbf{d_3}$) $\omega$ = 0.35; ($\mathbf{a_4}$)-($\mathbf{d_4}$) $\omega$ = 0.41, stimulus $\varphi_{ext} = A\cos(\omega t) + B\cos(N\omega t)$

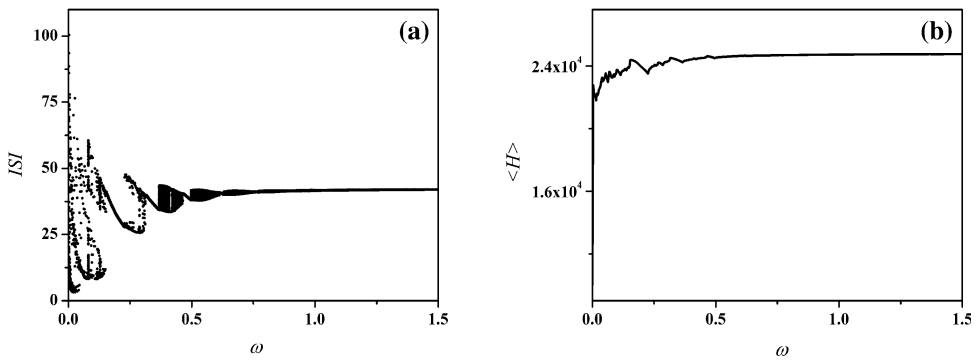


**Fig. 10** **a** Bifurcation diagram associated with the angular frequency of electromagnetic radiation. **b** Evolution of the average energy function with the angular frequency of electromagnetic radiation. External stimulus $\varphi_{ext} = A\cos(\omega t) + B\cos(N\omega t)$ with $A = 3.0$, $B = 3.0$, $N = 10$

slightly modulates the discharge rhythm at a fixed amplitude.

## Conclusions

In summary, when the periodic current or high-low frequency electromagnetic radiation is imposed on the Izhikevich neuron under electromagnetic induction, the transformation of electrical activity and Hamilton energy is investigated by changing external stimulus in this paper.

It is found that periodic current or electromagnetic radiation can induce multiple modes transition (e.g. spiking state, busting state, and chaotic states) in electrical activity, and the Hamiltonian energy is more dependent on the discharge mode. In particular, there is a distinct shift and transition in Hamiltonian energy when the discharge mode is switched quickly. The average Hamilton energy decreases when the electrical activity changes from low rhythm into high rhythm, and the potential mechanism may be that the energy carried by each action potential decreases due to the restriction of energy conservation. In addition, it is found that the influence of high frequency amplitude $B$ on neurons is smaller than that of low frequency amplitude $A$ under electromagnetic radiation. The amplitude of stimulus signal has a greater effect on neuronal energy compared to the angular frequency, and the underlying mechanism may be that the stimulus signal with a larger amplitude (or strength) can inject sufficient energy to induce multiple modes transition in electrical activities, while angular frequency only slightly modulates the discharge rhythm at a fixed amplitude.

Our results may help better understand the relationship between electrical activity and energy, and understand the paroxysmal mechanism of epilepsy symptoms. Epilepsy is a type of chronic brain dysfunction caused by sudden abnormal discharge of neurons. The average Hamilton energy can be significantly decreased when the neuron is in bursting and chaotic states, which may indicate that paroxysmal epilepsy will release large energy quickly before restoring normal discharge behavior. Various noises (e.g. Gaussian white noise, channel noise, etc..) and network structure in nervous system can also affect the electrical activity and energy. Therefore, the effects of noise and signal on electrical activity and energy based on multilayer neural network of Izhikevich neuronal model under electromagnetic induction could be investigated in further works.

**Acknowledgements** This work was supported by the National Natural Science Foundation of China under Grant under Nos. 11775091(YJ), 11672122 and 11765011(JM).

## References

Carpenter CJ (1999) Electromagnetic induction in terms of the Maxwell force instead of magnetic flux. IEE Proceedings-Science, Measurement and Technology 146(4):182–193

Chua L (1971) Memristor-the missing circuit element. IEEE Trans Circuit Theory 18(5):507–519

Farokhniaee A, Large EW (2017) Mode-locking behavior of Izhikevich neurons under periodic external forcing. Phys Rev E 95:062414

FitzHugh R (1961) Impulses and physiological states in theoretical models of nerve membrane. Biophys J 1(6):445–466

Ge M, Jia Y, Kirunda JB, Xu Y, Shen J, Lu L, Liu Y, Pei Q, Zhan X, Yang L (2018) Propagation of firing rate by synchronization in a feed-forward multilayer Hindmarsh–Rose neural network. Neurocomputing 320:60–68

Ge M, Jia Y, Xu Y, Lu L, Wang H, Zhao Y (2019a) Wave propagation and synchronization induced by chemical autapse in chain Hindmarsh–Rose neural network. Appl Math Comput 352:136–145

Ge M, Lu L, Xu Y, Zhan X, Yang L, Jia Y (2019b) Effects of electromagnetic induction on signal propagation and synchronization in multilayer Hindmarsh–Rose neural networks. Eur Phys J Spec Top 228:2455–2464

Ge M, Jia Y, Lu L, Xu Y, Wang H, Zhao Y (2020a) Propagation characteristics of weak signal in feedforward Izhikevich neural networks. Nonlinear Dyn 99:2355–2367

Ge M, Lu L, Xu Y, Mamatimin R, Pei Q, Jia Y (2020b) Vibrational mono-/bi-resonance and wave propagation in FitzHugh–Nagumo neural systems under electromagnetic induction. Chaos, Solitons Fractals 133:109645

Gong PL, Xu JX (2001) Global dynamics and stochastic resonance of the forced FitzHugh–Nagumo neuron model. Phys Rev E 63(3):031906

Guo D, Li C (2009) Stochastic and coherence resonance in feed-forward-loop neuronal network motifs. Phys Rev E 79(5):051921

Hindmarsh JL, Rose RM (1982) A model of the nerve impulse using two first-order differential equations. Nature 296(5853):162–164

Hodgkin AL, Huxley AF (1952) A quantitative description of membrane current and its application. J Physiol 117:500–544

Izhikevich EM (2003) Simple model of Spiking Neurons. IEEE Trans Neural Netw 14(6):1569–1572

Izhikevich EM (2004) Which model to use for cortical spiking neurons? IEEE Trans Neural Netw 15(5):1063–1070

Kobe DH (1986) Helmholtz's theorem revisited. Am J Phys 54(6):552–554

Laughlin SB, Sejnowski TJ (2003) Communication in neuronal networks. Science 301(5641):1870–1874

Liu Y, Ma J, Xu Y, Jia Y (2019) Electrical mode transition of hybrid neuronal nodel induced by external stimulus and electromagnetic induction. Int J Bifurc Chaos 29(11):1950156

Lu L, Jia Y, Kirunda JB, Xu Y, Ge M, Pei Q, Yang L (2019a) Effects of noise and synaptic weight on propagation of subthreshold excitatory postsynaptic current signal in a feed-forward neural network. Nonlinear Dyn 95(2):1673–1686

Lu L, Jia Y, Xu Y, Ge M, Yang L, Zhan X (2019b) Energy dependence on modes of electric activities of neuron driven by different external mixed signals under electromagnetic induction. Sci China Technol Sci 62(3):427–440

Lu L, Bao C, Ge M, Xu Y, Yang L, Zhan X, Jia Y (2019c) Phase noise-induced coherence resonance in three dimension memristive Hindmarsh-Rose neuron model. Eur Phys J Special Top 228:2101–2110

Lu L, Jia Y, Ge M, Xu Y, Li A (2020) Inverse stochastic resonance in Hodgkin–Huxley neural system driven by Gaussian and non-Gaussian colored noises. Nonlinear Dyn. https://doi.org/10.1007/s11071-020-05492-y

Lv M, Ma J (2016) Multiple modes of electrical activities in a new neuron model under electromagnetic radiation. Neurocomputing 205:375–381

Lv P, Hu X, Lv J, Han J, Guo L, Liu T (2014) A linear model for characterization of synchronization frequencies of neural networks. Cogn Neurodyn 8(1):55–69

Lv M, Wang C, Ren G, Ma J, Song X (2016) Model of electrical activity in a neuron under magnetic flow effect. Nonlinear Dyn 85(3):1479–1490

Ma J, Song X, Tang J, Wang C (2015) Wave emitting and propagation induced by autapse in a forward feedback neuronal network. Neurocomputing 167:378–389

Ma J, Lv M, Zhou P, Xu Y, Tasawar H (2017) Phase synchronization between two neurons induced by coupling of electromagnetic field. Appl Math Comput 307:321–328

Mondal A, Upadhyay RK, Ma J, Yadav BK, Sharma SK, Mondal A (2019) Bifurcation analysis and diverse firing activities of a modified excitable neuron model. Cogn Neurodyn 13(4):393–407

Morris C, Lecar H (1981) Voltage oscillations in the barnacle giant muscle fiber. Biophys J 35(1):193–213

Parastesh F, Rajagopal K, Karthikeyan A, Alsaedi A, Hayat T, Pham VT (2018) Complex dynamics of a neuron model with discontinuous magnetic induction and exposed to external radiation. Cogn Neurodyn 12(6):607–614

Rostami Z, Jafari S (2018) Defects formation and spiral waves in a network of neurons in presence of electromagnetic induction. Cogn Neurodyn 12(2):235–254

Song XL, Jin WY, Ma J (2015) Energy dependence on the electric activities of a neuron. Chin Phys B 24(12):128710

Strukov DB, Snider GS, Stewart DR, Williams RS (2008) The missing memristor found. Nature 453(7191):80–83

Ullner E, Zaikin A, García O, Báscnoes R, Kurths J (2003) Vibrational resonance and vibrational propagation in excitable systems. Phys Lett A 312(5–6):348–354

Wang Z, Wang R (2014) Energy distribution property and energy coding of a structural neural network. Front Comput Neurosci 8:14

Wang R, Zhang Z (2007) Energy coding in biological neural network. Cogn Neurodyn 1(3):203–212

Wang R, Zhu Y (2016) Can the activities of the large scale cortical network be expressed by neural energy? A brief review. Cogn Neurodyn 10(1):1–5

Wang R, Zhang Z, Chen G (2008) Energy function and energy evolution on neural population. IEEE Trans Neural Netw 19(3):535–538

Wang R, Zhang Z, Chen G (2009) Energy coding and energy functions for local activities of the brain. Neurocomputing 73(1–3):139–150

Wang R, Tsuda I, Zhang Z (2015a) A new work mechanism on neuronal activity. Int J Neural Syst 25(03):1450037

Wang Z, Wang R, Fang R (2015b) Energy coding in neural network with inhibitory neurons. Cogn Neurodyn 9(2):129–144

Wang C, Wang Y, Ma J (2016) Calculation of Hamilton energy function of dynamical system by using Helmholtz theorem. Acta Phys Sin 65(24):240501

Wang Y, Wang C, Ren G, Tang J, Jin W (2017a) Energy dependence on modes of electric activities of neuron driven by multi-channel signals. Nonlinear Dyn 89:1967–1987

Wang Y, Wang R, Zhu Y (2017b) Optimal path-finding through mental exploration based on neural energy field gradients. Cogn Neurodyn 11(1):99–111

Wang R, Wang Z, Zhu Z (2018) The essence of neuronal activity from the consistency of two different neuron models. Nonlinear Dyn 92(3):973–982

Wilson HR (1999) Simplified dynamics of human and mammalian neocortical neurons. J Theor Biol 200(4):375–388

Wu FQ, Ma J, Zhang G (2019) Energy estimation and coupling synchronization between biophysical neurons. Sci China Technol Sci 1:2. https://doi.org/10.1007/s11431-019-9670-1

Xu Y, Ying H, Jia Y, Ma J, Hayat T (2017) Autaptic regulation of electrical activities in neuron under electromagnetic induction. Sci Rep 7:43452

Xu Y, Jia Y, Ge M, Lu L, Yang L, Zhan X (2018a) Effects of ion channel blocks on electrical activity of stochastic Hodgkin-Huxley neural network under electromagnetic induction. Neurocomputing 283:196–204

Xu Y, Jia Y, Kirunda JB, Shen J, Ge M, Lu L, Pei Q (2018b) Dynamic behaviors in coupled neuron system with the excitatory and inhibitory autapse under electromagnetic induction. Complexity 2018:3012743

Xu Y, Jia Y, Wang H, Liu Y, Wang P, Zhao Y (2019a) Spiking activities in chain neural network driven by channel noise with field coupling. Nonlinear Dyn 95(4):3237–3247

Xu Y, Ma J, Zhan X, Yang L, Jia Y (2019b) Temperature effect on memristive ion channels. Cogn Neurodyn 13:601–611

Yao Y, Ma J (2018) Weak periodic signal detection by sine-Wiener-noise-induced resonance in the FitzHugh-Nagumo neuron. Cogn Neurodyn 12(3):343–349

Zaikin AA, López L, Baltanás JP, Kurths J, Sanjuán MAF (2002) Vibrational resonance in a noise-induced structure. Phys Rev E 66(1):011106

Zhao J, Deng B, Qin Y, Men C, Wang J, Wei X, Sun J (2016) Weak electric fields detectability in a noisy neural network. Cogn Neurodyn 11(1):81–90

Zhu Z, Wang R, Zhu F (2018) The energy coding of a structural neural network based on the Hodgkin–Huxley model. Front Neurosci 12:122

Zhu F, Wang R, Pan X, Zhu Z (2019) Energy expenditure computation of a single bursting neuron. Cogn Neurodyn 13:75–87

**Publisher's Note** Springer Nature remains neutral with regard to jurisdictional claims in published maps and institutional affiliations.